9684 *Inorg. Chem.* **2009**, *48*, 9684–9692
DOI: 10.1021/ic900479w

Inorganic Chemistry
Article

Photooxidation of a Platinum-Anthracene Pincer Complex: Formation and Structures of Pt^{II}-Anthrone and -Ketal Complexes

Jian Hu, Huan Xu, Minh-Hai Nguyen, and John H. K. Yip*

Department of Chemistry, National University of Singapore, 3 Science Drive 3, Singapore 11754

Received March 13, 2009

Irradiating the cyclometalated pincer complex Pt^{II}(DPA)Cl (**1**, DPA = 1,8-bis(diphenylphosphino)anthracene) in the presence of O_2 led to three sequential oxidations of the anthracenyl ring. The first photoproduct, a Pt^{II}-9, 10-endoperoxide complex, was converted photochemically to a Pt^{II}-9-hydroxyanthrone complex **A** which was further oxygenated to a Pt^{II}-hemiketal (**B**). The oxidation of **A**, which could be accelerated by light irradiation, probably involved a Pt^{II}-anthraquinone intermediate. **B** underwent acid-catalyzed ketalization to form a binuclear Pt^{II}_2-diketal (**B1**). The photolysis was followed by UV−vis absorption and NMR spectroscopy, and the structures of **A** and **B1** were characterized by single crystal X-ray diffraction.

Introduction

Photooxidation has important applications in catalysis, oxidation of biomolecules and organic synthesis.[1] Many photooxidations involve oxygen in its lowest energy singlet excited state ($^1\Delta_g$) which is usually produced by energy transfer from an electronic excited state of a dye to the triplet ground state of oxygen ($^3\Sigma_g^-$).[2] Reactions of $^1O_2$ and organic molecules such as polycyclic aromatics, olefins, and heterocyclics have been well examined.[3] A paradigmatic example related to the present study is photooxidation of anthracene in which $^1O_2$ undergoes cycloaddition with the polycyclic compound to give 9,10-endoperoxide (**EP**) as the primary photoproduct.[2a,4]

While photooxygenation of organic molecules has been extensively studied, the scope of photooxygenation of transition metal complexes is rather limited even though many emissive metal complexes can photosensitize O_2 efficiently.[5] Most of the studies focused on thiolate complexes,[6] especially d^8 square planar M^{II}-*cis*-dithiolates (M = Ni^{II}, Pd^{II}, Pt^{II}). Except the photooxidation of (dibutyl-2,2′-bipyridine)Pt^{II}-(1,2-diphenyl-1,2-ethanedithiolate)[6a] in which the dithiolate was dehydrogenated, reactions between metal−thiolates and $^1O_2$ led to oxidation of the coordinated sulfur atoms to sulfinate (O═S═O).

Interactions between metal and organic chromophores can influence the photophysics and the photochemistry of the latter.[7] Our recent study showed that attaching Pt^{II} ion to

*To whom correspondence should be addressed. E-mail: chmyiphk@nus.edu.sg. Fax: 65-67791691.

(1) (a) Maldotti, A.; Molinari, A.; Amadelli, R. *Chem. Rev.* **2002**, *102*, 3811. (b) Meunier, B. *Chem. Rev.* **1992**, *92*, 1411. (c) Foote, C. S. *Oxygen Oxy-Radicals Chem. Biol.* **1981**, 425. (d) George, M. V.; Bhat, V. *Chem. Rev.* **1979**, *79*, 447.

(2) (a) Foote, C. S.; Wexler, S. *J. Am. Chem. Soc.* **1964**, *86*, 3879. (b) Foote, C. S. *Acc. Chem. Res.* **1968**, *1*, 104–110. (c) Greer, A. *Acc. Chem. Res.* **2006**, *39*, 797.

(3) (a) Adam, W.; Griesbeck A. G. In *CRC Handbook of Organic Chemistry and Photobiology*; Horspool, W.M., Song, P.-S., Eds.; CRC Press Inc.: London 1995; pp 311−324. (b) Foote, C. S. *Pure Appl. Chem.* **1971**, *45*, 635. (c) Sivaguru, J.; Solomon, M. R.; Poon, T.; Jockusch, S.; Bosio, S. G.; Adam, W.; Turro, N. J. *Acc. Chem. Res.* **2008**, *41*, 387. (d) Clennan, E. L. *Tetrahedron* **1991**, *47*, 1343.

(4) (a) Corey, E. J.; Taylor, W. C. *J. Am. Chem. Soc.* **1964**, *86*, 3881. (b) Aubry, J.-M.; Pierlot, C.; Rigaudy, J.; Schmidt, R. *Acc. Chem. Res.* **2003**, *36*, 668. (c) Sparfel, D.; Gobert, F.; Rigaudy, J. *Tetrahedron* **1980**, *36*, 2225.

(5) (a) Gafney, H. D.; Adamson, A. W. *J. Am. Chem. Soc.* **1972**, *94*, 8238. (b) Szaciłowski, K.; Macyk, W.; Drzewiecka-Matuszek, A.; Brindell, M.; Stochel, G. *Chem. Rev.* **2005**, *105*, 2647. (c) Demas, J. M.; Harris, E. W.; McBride, R. P. *J. Am. Chem. Soc.* **1977**, *99*, 3547. (d) Djurovich, P. I.; Murphy, D.; Thompson, M. E.; Hernandez, B.; Gao, R.; Hunt, P. L.; Selke, M. *Dalton Trans.* **2007**, *34*, 3763. (e) Abdel-Shafi, A. A.; Worrall, D. R.; Ershov, A. Y. *Dalton Trans.* **2004**, 30. (f) Muro, M. L.; Diring, S.; Wang, X.; Ziessel, R.; Castellano, F. N. *Inorg. Chem.* **2008**, *47*, 6796. (g) Liu, Y.; Hammitt, R.; Lutterman, D. A.; Joyce, L. E.; Thummel, R. P.; Turro, C. *Inorg. Chem.* **2009**, *48*, 375. (h) Mulazzani, Q. G.; Sun, H.; Hoffman, M. Z.; Ford, W. E.; Rodgers, M. A. J. *J. Phys. Chem.* **1994**, *98*, 1145.

(6) (a) Zhang, Y.; Ley, K. D.; Schanze, K. S. *Inorg. Chem.* **1996**, *35*, 7102. (b) Connick, W. B.; Gray, H. B. *J. Am. Chem. Soc.* **1997**, *119*, 11620. (c) Galvez, C.; Ho, D. G.; Azod, A.; Selke, M. *J. Am. Chem. Soc.* **2001**, *123*, 3381. (d) Anbalagan, V.; Srivastava, T. S. *J. Photochem. Photobiol., A: Chem.* **1995**, *89*, 113. (e) Anbalagan, V.; Srivastava, T. S. *J. Photochem. Photobiol., A: Chem.* **1994**, *77*, 141. (f) Anbalagan, V.; Srivastava, T. S. *Polyhedron* **1994**, *13*, 291. (g) Farmer, P. J.; Solouki, T.; Mills, D. K.; Soma, T.; Russell, D. H.; Reibenspies, J. H.; Darensbourg, M. Y. *J. Am. Chem. Soc.* **1992**, *114*, 4601. (h) Darensbourg, M. Y.; Tuntulani, T.; Reibenspies, J. H. *Inorg. Chem.* **1995**, *34*, 6287.

(7) (a) Sayer, P.; Gouterman, M.; Connell, C. R. *Acc. Chem. Res.* **1982**, *15*, 73. (b) Wrighton, M. S.; Morse, D. L; Pdungsap, L. *J. Am. Chem. Soc.* **1975**, *97*, 2073. (c) Lee, P. H.-M.; Ko, C. C.; Zhu, N.; Yam, V. W.-W. *J. Am. Chem. Soc.* **2007**, *129*, 6058. (d) Hu, J.; Lin, R.; Yip, J. H. K.; Wong, K.-Y.; Ma, D.-L.; Vittal, J. J. *Organometallics* **2007**, *26*, 6533. (e) Heng, W. Y.; Hu, J.; Yip, J. H. K. *Organometallics* **2007**, *26*, 6760. (f) Hu, J.; Yip, J. H. K.; Ma, D.-L.; Wong, K.-Y.; Chung, W.-H. *Organometallics* **2009**, *28*, 51. (g) Wang, B.-Y.; Karikachery, A. R.; Li, Y.; Singh, A.; Lee, H. B.; Sun, W.; Sharp, P. R. *J. Am. Chem. Soc.* **2009**, *131*, 3150. (h) Partyka, D. V.; Esswein, A. J.; Zeller, M.; Hunter, A. D.; Gray, T. G. *Organometallics* **2007**, *26*, 3279.

Published on Web 09/23/2009

anthracene changes the electronic spectroscopy of the organic chromophore significantly.[7d,e] This led us to contemplate the effect of metals on excited state chemistry of anthracene, especially the well-known photooxygenation. In search for a system suitable for studying photooxidation of metal-anthracene, our attention was drawn to the pincer complex Pt^{II}(DPA)X (X = Cl (**1**), Br (**2**), I (**3**), DPA = 1,8-bis(diphenylphosphino)anthracene) (Scheme 1).[8] DPA and its cyclometalated Ni^{II} and Pd^{II} complexes were first synthesized by Haenel.[9] Our interest in the Pt^{II} pincer complex was aroused by the intriguing reactivity[10] and rich photochemistry[11] of Pt^{II} complexes. Most importantly, being attached to the anthracenyl ring at the C(9) position, the Pt^{II} ion can influence the course of the photooxidation. Indeed, the results of the present study showed that unlike the photooxidation of anthracene, which gives rise to **EP** and a myriad of secondary photoproducts and thermal products such as 10-hydroxyanthrone, anthraquinone, and diepoxides,[4c] photooxygenation of **1** produces three oxidized complexes sequentially.

Scheme 1

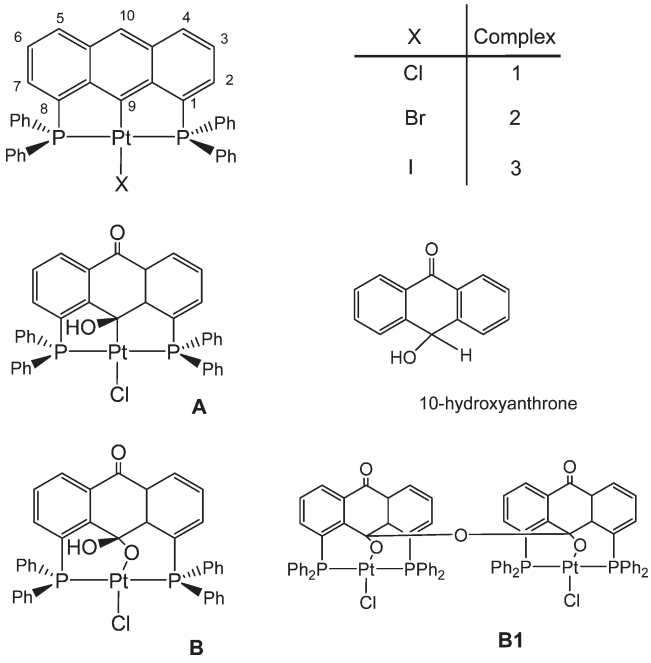

Experimental Section

General Method. All syntheses were carried out in N_2 atmosphere with standard Schlenck techniques. K_2PtCl_4 was purchased from Oxkem. $CHCl_3$ (GR) and $CDCl_3$ were used as received. 1,8-Difluoroanthracene[9b] and $NaPPh_2$[12] were prepared according to reported methods. The following chemicals were used as received: PPh_2Cl (Acros), 1,8-dichloroanthraquinone and CeF_2 (Aldrich). Anthracene (Aldrich) was used as standard for emission quantum yield and was purified by recrystallization from ethanol.

Physical Measurements. The UV/vis absorption and emission spectra of the complexes were recorded on a Hewlett-Packard HP8452A diode array spectrophotometer and a Perkin-Elmer LS-50D fluorescence spectrophotometer, respectively. Anthracene was used as a standard in measuring the emission quantum yields. ^1H and $^{31}P\{^1H\}$ NMR spectra were recorded at on either a Bruker ACF 300 or an AMX500 spectrometer. All chemical shifts are quoted relative to $SiMe_4$ (^1H) or H_3PO_4 (^{31}P). Elemental analyses of the complexes were carried out in the microanalysis laboratory in the Department of Chemistry at National University of Singapore.

Steady-State Photolysis. A LPS 300 SM xenon arc lamp controlled by LPS 300SM switched mode (75 to 300 W) was used as the light source in the photolysis. Optical filters were used to select the wavelength of the irradiation. For a typical photolysis, the power of the lamp was 80 W and the intensity of the incident light (λ = 300−500 nm) is 1.42×10^{-8} Einstein/s. Photolysis of NMR samples was carried out using xenon lamp with 300−500 nm filters. The UV−vis absorption changes were monitored by a Hewlett-Packard HP8452A diode array spectrophotometer. The quantum yields of the reactions were determined by ferrioxalate actinometry.[13] For preparative photolysis, solutions of metal complexes were irradiated by a tungsten lamp of 100 W.

Synthesis. Synthesis of 1, 8-Bis(diphenylphosphino)anthracene (DPA). A solution of 1,8-difluoroanthracene (1.20 g, 5.6 mmol) in 20 mL of 1,4-dioxane was slowly added into a solution $NaPPh_2$, which was prepared in situ by reacting sodium (1.25 g, 54 mmol) and excess PPh_2Cl (7.3 mL, 41 mmol) in refluxing 1,4-dioxane. The mixture was refluxed for 4 h and then cooled down to room temperature, followed by addition of ~10 mL of CH_3OH to quench excess $NaPPh_2$. All solvents were removed under vacuum; 100 mL of H_2O was then added to the resulting mixture, and the product was extracted with CH_2Cl_2 and purified by column chromatography (toluene/cyclohexane 10:1, v/v). The yellow solid obtained was washed with 2,2, 4-trimethylpentane to remove any $HPPh_2$. Yield: 1.97 g, 65%. Anal. Calcd (%) for $C_{38}H_{28}P_2$: C, 83.52; H, 5.13; Found (%): C, 84.12; H, 5.34. ^1H NMR ($CDCl_3$, 300 M Hz, δ/ppm): 9.77 (t, $^4J_{PH}$ = 5 Hz, 1H, H_9), 8.44 (s, 1H, H_{10}), 7.96 (d, $^3J_{HH}$ = 9 Hz, 2H, $H_{4,5}$), 7.49−7.44 (m, 2H, $H_{2,7}$), 7.33−7.23 (m, 20H, Ph), 7.03−6.99 (m, 2H, $H_{3,6}$). $^{31}P\{^1H\}$NMR ($CDCl_3$, 121.5 M Hz, δ/ppm): −14.06 (s). $^{13}C\{^1H\}$ NMR ($CDCl_3$, 75.48 M Hz, δ/ppm): 124.78 (t, $^3J_{C-P}$ = 27.9 Hz, C9), 125.97 (s, Ph C3), 128.31 (s, C10), 129.06, (d, $^1J_{C-P}$ = 7.5 Hz, C2,7), 129.29 (s, Ph C4), 129.91 (s, C4,5), 132.24 (d, $^3J_{C-P}$ = 3.8 Hz, C11,13), 132.71 (s, C3,6), 133. 91 (d, $^2J_{C-P}$ = 22.6 Hz, C8,14), 134.79 (d, $^2J_{C-P}$ = 20.4 Hz, Ph C2), 136.82 (d, $^1J_{C-P}$ = 15.3 Hz, C1, C8), 137.05 (d, $^1J_{C-P}$ = 10.6 Hz, Ph C1).

Synthesis of Pt^{II}(DPA)Cl (1). To a solution of K_2PtCl_4 (0.277 g, 0.667 mmol) in 80 mL of CH_3CN/H_2O (1:1, v/v) was added DPA (0.365 g, 0.668 mmol). The mixture was refluxed under N_2 for 18 h. The resulting yellow suspension was extracted with CH_2Cl_2. Addition of excess Et_2O to the concentrated extraction precipitated the product as yellow solids. Single crystals were obtained from vapor diffusion of Et_2O into its CH_2Cl_2 solution.

(8) During the preparation of this manuscript, Gelman et al reported the synthesis of Pt(DPA)Cl and its reaction with acetylene, see: Azerraf, C.; Shpruhman, A.; Gelman, D. *Chem. Commun.* **2009**, 466.

(9) (a) Haenel, M. W.; Jakubik, D.; Betz, P. *Chem. Ber.* **1991**, *124*, 333. (b) Haenel, M. W.; Oevers, S.; Bruckmann, J.; Kuhnigk, J.; Krüger, C. *Synlett* **1998**, 301.

(10) For reviews on pincer complexes, see: (a) van der Boom, M. E.; Milstein, D. *Chem. Rev.* **2003**, *103*, 1759. (b) Benito-Garagorri, D.; Kirchner, K. *Acc. Chem. Res.* **2008**, *41*, 201. (c) Gossage, R. A.; van de Kuil, L. A.; van Koten, G. *Acc. Chem. Res.* **1998**, *31*, 423. (d) Albrecht, M.; van Koten, G. *Angew. Chem., Int. Ed.* **2001**, *49*, 3750.

(11) (a) Jude, H.; Krause Bauer, J. A.; Connick, W. B. *J. Am. Chem. Soc.* **2003**, *125*, 3446. (b) Harkins, S. B.; Peters, J. C. *Inorg. Chem.* **2006**, *45*, 4316. (c) Du, P.; Knowles, K.; Eisenberg, R. *J. Am. Chem. Soc.* **2008**, *130*, 12576. (d) Wong, K. M.-C.; Yam, V. W.-W. *Coord. Chem. Rev.* **2007**, *251*, 2477. Lai, S.-W.; Che, C.-M. *Top. Curr. Chem.* **2004**, *241*, 27. (e) Shavaleev, N.; Adams, H.; Best, J.; Edge, R.; Navaratnam, S.; Weinstein, J. A. *Inorg. Chem.* **2006**, *45*, 9410. (f) Wan, K.-T.; Che, C.-M. *Chem. Commun.* **1990**, 140. (g) Hill, R. H.; Puddephatt, R. J. *J. Am. Chem. Soc.* **1985**, *107*, 1218.

(12) Kühl, O.; Sieler, J.; Baum, G.; Hey-Hawkins, E. *Z. Anorg. Allg. Chem.* **2000**, *626*, 605.

(13) Parker, C. A. *Proc. R. Soc. London, Ser. A* **1953**, *104*, 220.

Yield: 0.45 g, 87%. Anal. Calcd (%) for $C_{38}H_{27}ClP_2Pt \cdot CH_2Cl_2$: C, 54.40; H, 3.39; Found (%): C, 54.35; H, 3.05. ^{1}H NMR-($CDCl_3$, 500 M Hz, δ/ppm) 8.35 (t, $^5J_{Pt-H}$ = 2.4 Hz, 1H, H_{10}), 8.11 (d, J_{H-H} = 8.1 Hz, 2H, $H_{4,5}$), 7.95(m, 8H, phenyl H), 7.79(m, 2H, $H_{2,7}$), 7.54 (dd, J_{H-H} = J_{H-H} = 8.1 Hz, 2H, $H_{3,6}$), 7.48−7.43(m, 12H, Phenyl H). ^{31}P{^{1}H} NMR(121.5 M Hz, $CDCl_3$, δ/ppm): 40.22 (s, $^1J_{Pt-P}$ = 2995 Hz). ^{13}C{^{1}H} NMR ($CDCl_3$, 75.48 M Hz, δ/ppm): 121.33 (s, Ph, C3), 126.77 (s, C11,13), 129.41 (d, $^2J_{C-P}$ = 10.6 Hz, Ph C2), 129.40 (s, Ph C4), 131.52 (s, C3,6), 131.79 (d, $^1J_{C-P}$ = 40 Hz, C1,8), 134.61 (s, C4,5), 134.64 (d, $^2J_{C-P}$ = 13.4 Hz, C2,7), 134.56 (s, C10), 135.05 (d, $^1J_{C-P}$ = 150 Hz, Ph C1), 139.36, (s, C9), 143.36 (s, C12,14). FAB-MS: m/z (r.a.) 776 ([M]$^+$, 93%), 740.1([M − Cl]$^+$, 100%).

Synthesis of Pt^{II}(DPA)Br (2) and Pt^{II}(DPA)I (3). A mixture of **1** (0.10 g, 0.129 mmol) and excess KBr (0.5 g, 4.1 mmol) or KI (2 g, 12.1 mmol) was stirred in 80 mL CH_2Cl_2/MeOH (ratio is 1:1) at room temperature for 48 h. Yellowish solids were obtained after the solvent was evaporated. The solids were then extracted with CH_2Cl_2. The yellow solution was concentrated to 5 mL. Addition of excess diethyl ether to the solution precipitated the product as yellow solids. Crystals of both compounds were obtained from slow diffusion of hexane into a CH_2Cl_2 solution of the complexes. Yields for **2** and **3** are 43% and 57%, respectively. **2**: for $C_{39}H_{29}PtBrCl_2P_2$, Calcd (%) C, 51.73; H, 3.23; found (%); C, 51.24; H, 3.44. ^{1}H NMR ($CDCl_3$, 300 M Hz, δ/ppm): 8.38 (t, $^5J_{Pt,H}$ = 2.4 Hz, 1H, anthracene H_{10}), 8.10 (d, $J_{H,H}$ = 8.4 Hz, 2H, $H_{4,5}$), 7.97−7.88 (m, 8H, phenyl H), 7.75 (m, 2H, $H_{2,7}$), 7.51 (m, 2H, $H_{3,6}$), 7.48−7.24 (m, 12H, phenyl H). ^{31}P{^{1}H} NMR ($CDCl_3$, 121.5 MHz, δ/ppm): 40.31 (s, J_{Pt-P} = 2968 Hz). ^{13}C{^{1}H} NMR ($CDCl_3$, 75.48 M Hz, δ/ppm): 121.41 (s, Ph, C3), 126.90 (s, C11,13), 129.28 (d, $^2J_{C-P}$ = 10.2 Hz, Ph C2), 129.31 (s, Ph C4), 131.56 (s, C3,6), 131.89 (d, $^1J_{C-P}$ = 25.7 Hz, C1,8), 132.00 (s, C4,5), 134.63 (d, $^2J_{C-P}$ = 13.5 Hz, C2,7), 134.90 (d, $^1J_{C-P}$ = 75.5 Hz, Ph C1), 134.62 (s, C10), 139.93, (s, C9), 145.97 (s, C12,14). ESI MS: m/z 823 ([M]$^+$, 93%). **3**: for $C_{39}H_{29}PtICl_2P_2$. Calcd (%) C, 49.18; H, 3.06, found (%); C, 49.52; H, 3.32. ^{1}H NMR ($CDCl_3$, 300 MHz, δ/ppm): 8.44 (t, $^5J_{Pt,H}$ = 2.4 Hz, 1H, anthracene H_{10}), 8.11 (d, J_{H-H} = 7.6 Hz, 2H, $H_{4,5}$), 7.96−7.86 (m, 8H, phenyl H), 7.73(m, 2H, $H_{2,7}$), 7.51 (dd, J_{H-H} = J_{H-H} = 7.6 Hz, 2H, $H_{3,6}$), 7.48−7.25 (m, 12H, phenyl H). ^{31}P{^{1}H} NMR ($CDCl_3$, 121.5 M Hz, δ/ppm) 41.02 (s, J_{Pt-P} = 2926 Hz). ^{13}C{^{1}H} NMR ($CDCl_3$, 75.48 M Hz, δ/ppm): 121.47 (s, Ph, C3), 127.04 (s, C11,13), 129.12 (d, $^2J_{C-P}$ = 10.4 Hz, Ph C2), 129.15 (s, Ph C4), 131.57 (s, C3,6), 131.75 (d, $^1J_{C-P}$ = 52.8 Hz, C1,8), 134.84 (d, $^2J_{C-P}$ = 13.2 Hz, C2,7), 134.86 (s, C4,5), 134.11 (d, $^1J_{C-P}$ = 34.7 Hz, Ph C1), 134.86 (s, C10), 141.04, (t, $^3J_{C-P}$ = 26.4, $^1J_{C-Pt}$ = 110 Hz, C9), 145.56 (s, C12,14). ESI MS: m/z: 867 ([M]$^+$, 50%).

Photoproduct A. Compound **1** (0.05 g, 0.067 mmol) was dissolved in 20 mL of $CHCl_3$ and irradiated with a tungsten lamp (100 W) for 24 h. The resulting solution was filtered, and the solvent was removed by rotaevaporation. Solids obtained were dissolved in CH_3CN and filtered. Violet block crystals were obtained by slow diffusion of diethyl ether into a CH_3CN solution. Yield = 56%. $C_{46}H_{32}PtP_2$ Calcd (%): C, 65.55; H, 3.83. found (%); C, 65.38; H, 3.86. ^{1}H NMR($CDCl_3$, 500 M Hz, δ/ppm): 8.29 (dd, 2H, J_{H-H} = 7.4 Hz, $H_{4,5}$), 7.88 (m, 4H, Ph), 7.82(m, 4H, Ph), 7.71(m. 2H, $H_{2,7}$), 7.60 (dd, J=7.4 Hz, 2H, $H_{3,6}$), 7.48−7.43 (m, 12H, Ph), ^{31}P{^{1}H} NMR ($CDCl_3$, 121.5 MHz, δ/ppm): 39.34 (s), ($^1J_{Pt-P}$= 3171 Hz). ESI MS: m/z 851([M]$^+$, 100%). ^{13}C{^{1}H} NMR ($CDCl_3$, 75.48 M Hz, δ/ppm): 78.9 (s, platinated C(9)), 129.4−161.4 (aromatic C), 184.8 (s, ketone C).

Photoproduct B1·4CH_2Cl_2. It was synthesized by photolysis (Tungsten lamp, 100 W) of an aerated $CHCl_3$ solution of **A** for 2 days. The solvent was purified by fractional distillation to remove EtOH. The compound was isolated and purified by recrystallization from CH_2Cl_2/Et_2O. Yield = 62%. $C_{76}H_{52}Pt_2P_4O_5Cl_2$ Calcd (%): C, 56.00; H, 3.19. found (%); C, 56.81; H, 3.42. ^{1}H NMR (300 Mz, in $CDCl_3$, δ/ppm): 8.07 (d, J_{H-H} = 7 Hz, 2H, $H_{4,5}$), 7.90−7.83 (m, 4H, Ph), 7.51−7.42 (m, 18 H, Ph, $H_{2,7}$), 7.00−6.97 (m, 2H, $H_{3,6}$), 3.06 (s, 1H, OH). ^{31}P{^{1}H} NMR ($CDCl_3$, 121.5 MHz, δ/ppm): 18.57 (s, $^1J_{P-Pt}$ = 2870 Hz). ^{13}C{^{1}H} NMR ($CDCl_3$, 75.48 M Hz, δ/ppm): 97.5 (s, ketal C), 124.7−156.0 (aromatic C), 186.8 (s, ketone C).

X-ray Crystallography. The diffraction experiments were carried out on a Bruker AXS SMART CCD 3-circle diffractometer with a sealed tube at 223 K using graphite-monochromated Mo Kα radiation (λ = 0.71073 Å). The software used were SMART[13a] for collecting frames of data, indexing reflection and determination of lattice parameters; SAINT[14a] for integration of intensity of reflections and scaling; SADABS[14b] for empirical absorption correction; and SHELXTL[14c] for space group determination, structure solution, and least-squares refinements on $|F|$.[2] Anisotropic thermal parameters were refined for the rest of the non-hydrogen atoms. The hydrogen atoms were placed in their ideal positions. The crystallographic data and experimental details for **1**, **A**•CH_3CN and **B1**•4CH_2Cl_2 are given in the Table 1.

Results and Discussion

Synthesis. 1,8-bis(diphenylphosphino)anthracene (DPA) was first synthesized by Haenel et al.[9] Our work showed that treating 1,8-difluoroanthracene with excess $NaPPh_2$ afforded DPA in reasonably good yield (65%). The complex Pt(DPA)Cl (**1**) was synthesized by refluxing a CH_3CN/H_2O mixture of DPA and K_2PtCl_4. The bromide (**2**) and iodide (**3**) analogues were prepared from **1** by ligand substitution. All three complexes show a singlet with Pt satellites in their ^{31}P{^{1}H} NMR spectra. The chemical shifts ($\delta \sim 40$) and J_{Pt-P} constants (2926−2994 Hz) of the signals are similar.

Structures of Pt(DPA)X (X = Cl, Br, I). Figure 1 shows the X-ray crystal structure of **1**·CH_3CN (see Table 2 for selected structural parameters and Supporting Information for the structures of **2** and **3**). The structures of **1**, **2**, and **3** are very similar, all showing a 4-coordinated Pt ion bonded to the C(9) atom of the anthracenyl ring, the two P atoms at the 1,8-positions, and a halide ion that is *trans* to the metalated carbon atom.

The local geometry of the central Pt ion is distorted square planar in **1**−**3** and the anthracenyl ring is planar; in fact except the phenyl rings, all atoms of the molecule lie nearly on the same plane. The P−Pt−P angles (166.86(5)−167.34(3)°) in the complexes deviates from linearity, and the C−Pt−P angles are ~83.6°. The Pt−C (1.991(3)−2.015(5) Å) and Pt−P (2.2664(9)−2.2784(4) Å) bond distances are typical for Pt^{II}−PCP pincers.[15] The C−Pt−X angles are close to 180°. Despite the different *trans*-influence of the halides, the Pt−C distances in the complexes are rather close (1991(3), 1.997(4), and 2,015(5) Å for **1**, **2**, and **3**, respectively), indicating that it is fixed by the rigid pincer coordination. On the other hand, because of the strong *trans*-influence of the carbanion, the Pt−X distances (2.3914(9), 2.4799(6), 2.6645(5) Å for Cl, Br and I for X = Cl, Br, I) are consistently longer

(14) (a) *SMART & SAINT Software Reference Manuals*, version 4.0; Siemens Energy & Automation, Inc., Analytical Instrumentation: Madison, WI, 1996. (b) Sheldrick, G. M. *SADABS: A Software for Empirical Absorption Correction*; University of Göttingen: Göttingen, Germany, 1996. (c) *SHELXTL Reference Manual*, version 5.03; Siemens Energy & Automation, Inc., Analytical Instrumentation: Madison, WI, 1996.

(15) (a) Schwartsburd, L.; Poverenov, E.; Shimon, L. J. W.; Milstein, D. *Organometallics* **2007**, *26*, 2931. (b) Adams, J. L.; Arulsamy, N.; Roddick, D. M. *Organometallics* **2009**, *28*, 1148. (c) Poverenov, E.; Leitus, G.; Shimon, L. J. W.; Milstein, D. *Organometallics* **2005**, *24*, 5937.

Table 1

complex	**1**•CH_3CN	**A**•CH_3CN	**B1**•$4CH_2Cl_2$
empirical formula	$C_{40}H_{30}ClP_2Pt$	$C_{40}H_{30}ClNO_2P_2Pt$	$C_{80}H_{60}Cl_{10}O_5P_4Pt_2$
formula weight	817.13	849.13	1969.84
crystal system	monoclinic	orthorhombic	monoclinic
space group	$P2_1/n$	*Pbca*	*C*2/*c*
unit cell dimensions	a = 12.7731(6) Å	a = 18.7678(6) Å	a = 29.565(2) Å
	b = 17.7800(8) Å	b = 16.9665(6) Å	b = 12.9527(7) Å
	c = 14.4478(7) Å	c = 21.6485(8) Å	c = 23.9535(15) Å
	α = 90°	α = 90°	α = 90°
	β = 96.539(1)°	β = 90°	β = 125.014(1)°
	γ = 90°	γ = 90°	γ = 90°
volume (Å^3)	3259.8(3)	6893.4(4)	7512.8(8)
Z	4	8	4
density (calculated, g cm^{-3})	1.665	1.636	1.742
Absorption coefficient (mm^{-1})	4.515	4.278	4.214
F(000)	1608	3344	3864
crystal size (mm^3)	0.20 × 0.20 × 0.14	0.40 × 0.30 × 0.12	0.10 × 0.06 × 0.04
θ range for data collection	1.82 to 27.50°	1.87 to 27.50°	1.68 to 27.50°
index ranges	$-16 \le h \le 16$	$-24 \le h \le 24$	$-34 \le h \le 38$
	$-21 \le k \le 23$	$-22 \le k \le 22$	$-12 \le k \le 16$
	$-15 \le l \le 18$	$-28 \le l \le 28$	$-31 \le l \le 29$
Reflections collected	22701	86389	26185
independent reflections	7470 [R(int) = 0.0439]	7920 [R(int) = 0.0544]	8608 [R(int) = 0.0460]
max. and min transmission	0.5705 and 0.4654	0.6278 and 0.2795	0.8495 and 0.6780
data/restraints/parameters	7470/0/526	7920/0/426	8608/8/456
Goodness-of-fit (GOF)[b]	1.007	1.236	1.067
final R indices[a][$I > 2\sigma(I)$]	$R1$ = 0.0315, $wR2$ = 0.0637	$R1$ = 0.0404, $wR2$ = 0.0934	$R1$ = 0.0561, $wR2$ = 0.1555
largest diff. peak and hole (e Å^{-3})	1.102 and −0.770	3.621 and −1.428	2.054 and −2.010

[a] $R1 = \sum||F_o| - |F_c||/\sum|F_o|$; $wR2 = [\sum w(F_o^2 - F_c^2)^2/\sum w(F_o^4)]^{1/2}$. [b] GOF = $[\sum[w(F_o^2 - F_c^2)^2]/(n-p)]^{1/2}$. For all crystal determinations, scan type and wavelength of radiation used are ω and 0.71073 Å, respectively.

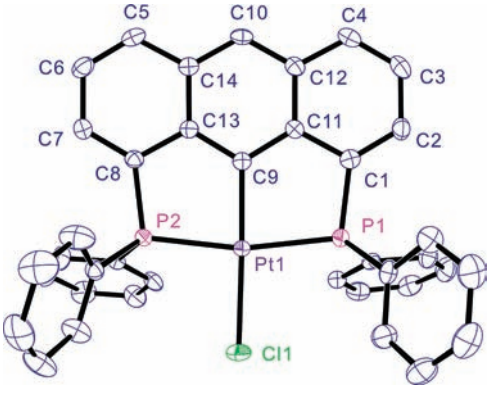

Figure 1. ORTEP plot of **1**·CH_3CN (thermal ellipsoids are drawn with 50% probability). The hydrogen atoms and solvent are omitted for clarity.

Table 2. Selected Bond Lengths and Angles **Pt(DPA)Cl**•CH_3CN

Pt(1)−C(9)	1.991(3)	C(9)−Pt(1)−P(2)	83.79(10)
Pt(1)−P(2)	2.2664(9)	P(1)−Pt(1)−P(2)	167.34(3)
Pt(1)−Cl(1)	2.3914(9)	C(9)−Pt(1)−Cl(1)	177.54(10)
		P(2)−Pt(1)−Cl(1)	94.53(3)

than the corresponding bonds in $Pt^{II}X_4^{2-}$ (2.308(2), 2.418(9), and 2.606(2) Å).[16]

Electronic Spectroscopy. Figure 2 shows the UV−vis absorption spectra of the Pt^{II}-complexes and DPA. The absorption spectra of the complexes are very similar, all showing a moderately intense vibronic band in 390−480 nm (λ_{max} = 454 nm, ε_{max} =7.6−9.2 × 10^3 M^{-1} cm^{-1}), and a very intense band at ∼280 nm (ε_{max} = 5.2−5.9 × 10^4 M^{-1} cm^{-1}). Both anthracene (λ_{max} = 255 nm, 358 nm) and DPA (λ_{max} = 266 nm, 380 nm) show similar absorption bands, suggesting that the spectra are dominated by $\pi \rightarrow \pi^*$ transitions of the anthracenyl rings.[17] Notably, there is a progressive red-shift of the absorptions from anthracene to DPA to the Pt complexes: the vibronic bands of DPA and **1** are shifted from that of anthracene by 1580 cm^{-1} and 4430 cm^{-1}, respectively. It indicates increasing perturbations of the electronic structures of the anthracenyl ring as it is substituted first with PPh_2 groups and then the Pt^{II} ion. No distinct metal-to-ligand-charge-transfer (MLCT) or ligand-to-ligand-charge-transfer (LLCT) band is found in the spectra as they are probably masked by the intense ligand-centered transitions.

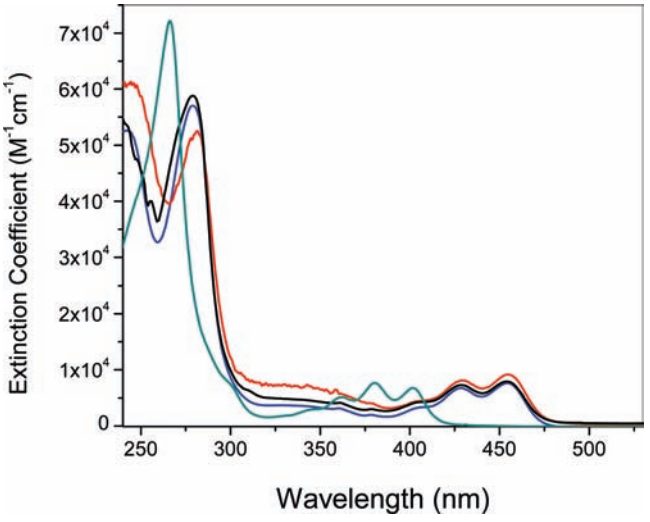

Figure 2. UV−vis absorption spectra of DPA (green), **1** (black), **2** (blue), and **3** (red) in CH_2Cl_2 at 298 K.

(16) (a) Britten, J.; Lock, C. J. L. *Acta Crystallogr. B* **1979**, *35*, 3065. (b) Melanson, R.; Rochon, F. D.; Hubert, J. *Acta Crystallogr. B* **1979**, *35*, 736. (c) Olsson, L. F.; Oskarsson, A. *Acta Chem. Scand.* **1989**, *43*, 811.

(17) (a) Kessinger, M.; Michl, J. *Excited States and Photochemistry of Organic Molecules*; VCH: New York, 1995. (b) Turro, N. J. *Modern Molecular Photochemistry*; Benjamin: Menlo Park, 1978.

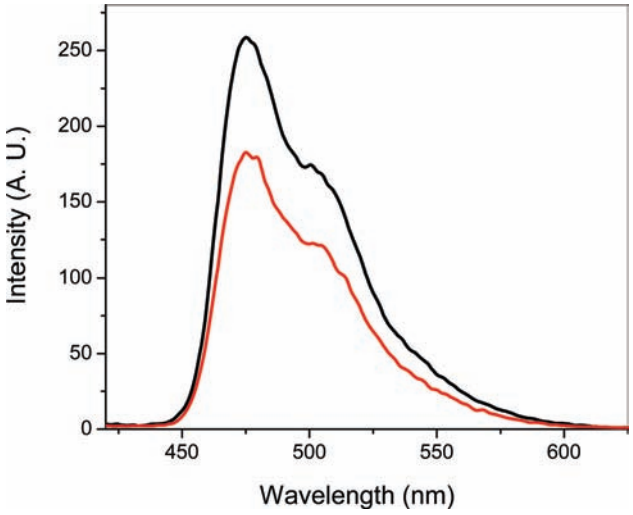

Figure 3. Emission spectra of **1** in a degassed CH_2Cl_2 solution (black) and in an oxygen-saturated CH_2Cl_2 solution (red) at room temperature (excitation wavelength = 390 nm).

However, in the C_{2v} symmetry of the complexes, the $5d_{xz}$ and the $6p_z$ orbitals of the Pt^{II} ion and the np_z (n = 3, 4, or 5) orbital of the halide have b_1 symmetry as the highest occupied molecular orbital (HOMO) and the lowest unoccupied molecular orbital (LUMO) of the anthracenyl ring.[18] It is expected that mixing of the orbitals would introduce MLCT and LLCT character to the $\pi\rightarrow\pi^*$ transitions.

Emission. The Pt complexes are luminescent in solution and solid state at room temperature. Irradiating degassed CH_2Cl_2 solutions of the complexes at 390 nm give emissions at λ_{max} = 474 nm (Figure 3) with vibronic shoulder at 520 nm. The small Stokes shift (~900 cm^{-1}) between the emission and the $\pi\rightarrow\pi^*$ absorption suggests the emission arises from the lowest energy $\pi\pi^*$ excited state of the anthracenyl ring. The complex **1** displays strong emission in degassed CH_2Cl_2 with quantum yield of 0.22.

The emissions of the complexes can be quenched by oxygen. Bubbling O_2 into a CH_2Cl_2 solution of **1** for 15 min reduces the emission intensity to ~70% of that of the degassed solution. The fluorescence restores nearly to its original intensity after removal of oxygen by freeze–pump–thaw cycles.

Photolysis of 1. Upon irradiation (λ = 300–500 nm), an oxygen-saturated $CHCl_3$ solution of **1** turned from yellow to purple. Figure 4 shows the UV–vis spectral changes during photolysis. "Wet chloroform" containing adventitious water was used as solvent for the photolysis. It was shown later that water took part in the formation of photoproducts.

The vibronic $\pi\rightarrow\pi^*$ band in 390–480 nm disappeared in 1 h. Concurrently, two weak absorption bands at 538 and 706 nm developed. The bleaching of the anthracenyl $\pi\rightarrow\pi^*$ transitions indicates the π-conjugation of the anthracenyl ring is partially disrupted. No isosbestic point was observed in the overlaid spectra, indicating that more than one species was produced in the photochemical reaction.

(18) The short and long axes of the anthracenyl ring are defined as x- and y-axes.

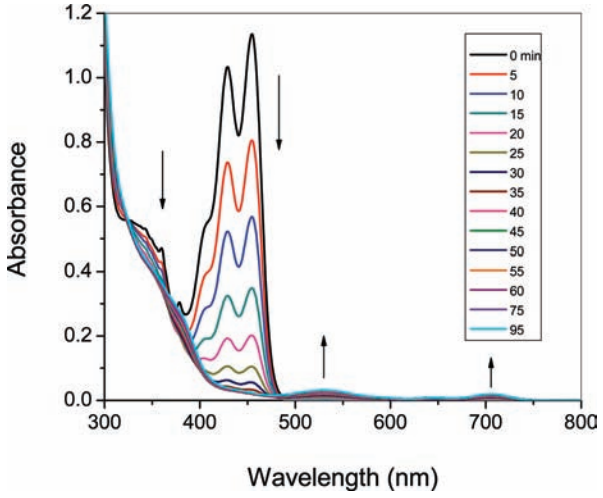

Figure 4. UV–visible absorption spectra of an air-saturated $CDCl_3$ solution of **1** at different irradiation time. Conditions: light intensity = 80 W, wavelength = 300–500 nm. The arrows indicate directions of absorbance changes.

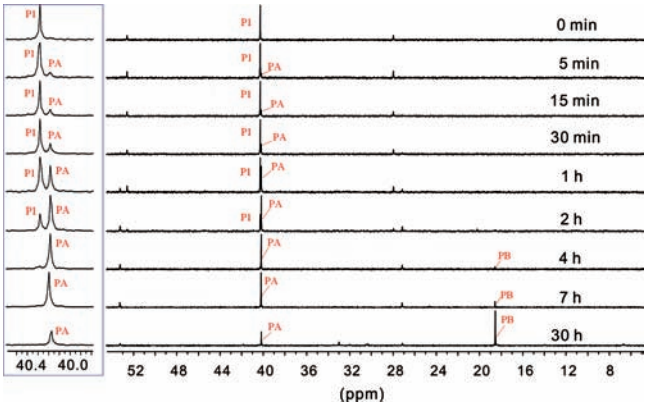

Figure 5. $^{31}P\{^1H\}$ NMR spectral changes during the photolysis of an oxygen-saturated $CDCl_3$ solution of **1** (irradiation wavelength = 300–500 nm, power = 80 W). Inset shows magnified **P1** and **PA**.

$^{31}P\{^1H\}$ NMR spectroscopy provided useful information about the photolysis (Figure 5). The starting complex **1** showed a singlet (labeled **P1**) at δ 40.22 ($^1J_{Pt-P}$ = 2995 Hz). A new singlet **PA** at δ 39.34 ($^1J_{Pt-P}$ = 3171 Hz) appeared after irradiation for 5 min. As the photolysis continued, the intensity of the **PA** grew at the expense of that of the **P1**. The **P1** completely disappeared after 4 h of irradiation and a new singlet **PB** at δ 18.57 ($^1J_{Pt-P}$ = 2870 Hz) started to appear. The intensity of the **PB** grew very slowly at the expense of that of the **PA**, and after 30 h of irradiation, the **PB** became the most intense signal. The species that give rise to the **PA** and the **PB** are labeled **A** and **B**, respectively. The results of the ^{31}P NMR experiment showed that the formation of **A** and **B** was sequential, that is, **1**→**A**→**B**. Clearly, both **A** and **B** are Pt-phosphine complexes as the **PA** and the **PB** display Pt satellites. Furthermore, since both signals are singlet, it implies the P atoms in each of the two complexes are equivalent, as confirmed later by the crystal structures of **A** and **B**.

The sequential formation of **A** and **B** was also observed in the ^1H NMR spectra of the photolysis (Supporting Information) which showed a new set of signals after

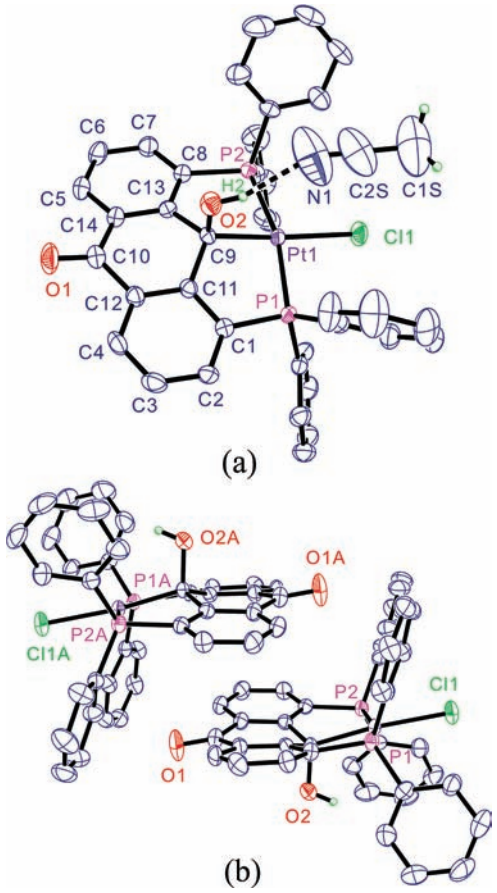

Figure 6. (a) ORTEP diagram of **A**·CH_3CN. Thermal ellipsoids are drawn with 50% probability. All the hydrogen atoms are omitted except the OH group. (b) Side-view showing the butterfly shape of the anthrone ligand and the stacking of the molecules. H atoms and MeCN were omitted.

Table 3. Selected Bond Lengths (Å) and Angles (deg) for **A**•CH_3CN

Pt(1)−C(9)	2.051(5)	C(9)−Pt(1)−P(2)	83.94(14)
Pt(1)−P(1)	2.2670(13)	C(9)−Pt(1)−Cl(1)	174.32(14)
Pt(1)−P(2)	2.2650(13)	P(1)−Pt(1)−P(2)	166.29(5)
Pt(1)−Cl(1)	2.3967(13)	P(1)−Pt(1)−Cl(1)	96.00(5)
C(9)−O(2)	1.487(6)	O(2)−C(9)−C(13)	104.3(4)
C(10)−O(1)	1.223(7)	O(2)−C(9)−C(11)	102.6(4)
		O(2)−C(9)−Pt(1)	108.6(3)
		C(11)−C(9)−C(13)	111.5(4)
		C(11)−C(9)−Pt(1)	114.2(3)
		C(13)−C(9)−Pt(1)	114.4(3)
		C(12)−C(10)−C(14)	116.5(5)

5 min of irradiation. Although the signals of **1** and **A** overlapped extensively in the aromatic region, the formation of **A** was shown by the appearance of a doublet of doublets at δ 8.29 (H4,5 of **A**) and disappearance of the signals for H10 (δ 8.35) and H4,5 (δ 8.11) of **1**. The signals of **1** vanished after 4 h, and prolonged photolysis saw weakening of the signals of **A** (i.e., dd at δ 8.29) and growth of signals belonging to **B**.

Structure of Photoproduct A. The photoproduct **A** was isolated and X-ray crystal analysis showed that it is a Pt^{II}-9-hydroxyanthrone pincer complex (Figure 6 and Table 3). To our knowledge, **A** is the first metal-anthrone complex ever synthesized and structurally characterized.

The structure confirmed that the photochemical reaction is an oxygenation in which two O atoms are introduced to the C(9) and C(10) positions of the anthracenyl ring. The C(10)−H bond in **1** is converted to a ketone carbonyl group C(10)═O(1). The two lateral rings of the anthrone are bent toward each other (dihedral angle = 15.3°). Similar conformation is found in other anthrones such as 10-bromoanthrone (dihedral angle = 16°).[19] While the C(9) remains coordinated to the Pt ion, it becomes four-coordinate with an additional hydroxyl group. Because of structural constraints imposed by the planar geometry of the Pt^{II} ion and the bent conformation of the anthrone, the bonding geometry of the metalated C atom deviates from the ideal geometry for sp^3 hybridization. For example, the O(2)−C(9)−C(11) and C(13)−C(9)−Pt(1) angles are 117.1(5) and 114.4(3), respectively. The hydroxyl group is hydrogen bonded to the N atom of a CH_3CN molecule (calcd N···H distance = 2.022 Å). The C(10)−O(1) distance of 1.223(7) Å is typical for C═O double bond and the C(9)−O(2) distance of 1.487(6) Å signifies a single bond. The central ring of the anthrone displays a boat conformation with the hydroxyl group occupying the pseudo-axial position and the carbonyl bond being tilted slightly away from the two lateral rings. The carbonyl C(10) atom and the C(9) atom in the central ring are located out of the planes defined by the other 4 carbon atoms by 0.158 and 0.380 Å (c.f. 0.12 and 0.19 Å for 10-bromoanthrone). The Pt^{II} ion is chelated by the two P atoms and the C(9) carbanion, forming a distorted square planar geometry. The Pt(1)−C(9) bond distance (2.051(5) Å) is in the range of normal Pt^{II}−C(sp^3) bond lengths (2.03−2.07 Å).

The C(9)−Pt(1)−Cl(1) axis is slightly tilted from the central C(9)−C(10) axis of the anthrone. Interactions between the Pt ion and the hydroxyl O atom seem possible as the atoms are separated by 2.892 Å, slightly shorter than the sum of the van der Waals radii of the two atoms (3.24 Å).

Structure of B1. As previously mentioned, prolonged photolysis gave the photoproduct **B** (δ 18.57, $^1J_{Pt-P}$ = 2870 Hz). However, a diketal derivative of **B**, **B1**·$4CH_2Cl_2$, was isolated by recrystallization of the product in CH_2Cl_2/Et_2O (Figure 7, Table 4). The structure of the complex shows a binuclear Pt^{II}_2 complex in which two anthrone units are joined by an unusual platinated diketal PtO−C−O(3)−C−OPt linkage. The two halves of the molecule are related by a C_2 axis passing through the central O(3) atom which is bonded to the C(9) and C(9A) atoms at the flagpole positions of the two anthrone rings.

Comparing the structures of **A** and **B1** shows that an oxygen atom O(2) is inserted in each Pt−C bond. The Pt−O(2) bond (1.996(4) Å) is slightly shorter than the one in a reported Pt^{II}-ketal complex (2.027(3) Å).[20] The Pt^{II} ion displays a severely distorted square planar geometry where the P−Pt−P angle facing the O(2) is 155.79(6)° only.

The bonding geometry of the flagpole carbon atom C(9) is distorted from ideal tetrahedral. The Pt−Cl bonds in **B1** (2.3022(19) Å) are shorter than the Pt−Cl bonds in **1** (2.3914(9) Å) and **A** (2.3967(13) Å), suggesting the

(19) Destro, R.; D'Alfonso, T. B.; Simonetta, M. *Acta Crystallogr. B* **1973**, *29*, 2214.
(20) Bergamini, P.; Marchesi, E.; Bertolasi, V.; Fogagnolo, M.; Scarpantonio, L.; Manfredini, S.; Vertuani, S.; Canella, A. *Eur. J. Inorg. Chem.* **2008**, 529.

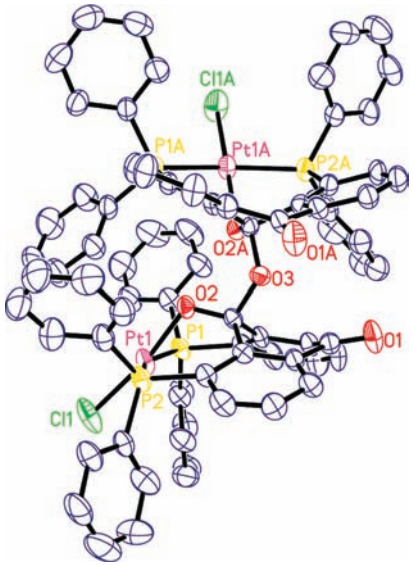

Figure 7. ORTEP plot of **B1**·$4CH_2Cl_2$ (30% thermal ellipsoids); H atoms and solvent molecules are omitted.

Table 4. Selected Bond Lengths (Å) and Angles (deg) for **B1**·$4CH_2Cl_2$

Pt(1)−P(1)	2.2991(17)	P(1)−Pt(1)−Cl(1)	99.23(7)
Pt(1)−O(2)	1.996(4)	P(1)−Pt(1)−P(2)	155.79(6)
Pt(1)−Cl(1)	2.3022(19)	P(1)−Pt(1)−O(2)	84.44(14)
C(9)−O(2)	1.363(7)	Cl(1)−Pt(1)−P(2)	97.14(7)
C(9)−O(3)	1.459(7)	Cl(1)−Pt(1)−O(2)	170.88(15)
C(10)−O(1)	1.210(8)	Pt(1)−O(2)−C(9)	114.4(4)
		C(9A)-O(3)−C(9)	123.3(6)
		O(2)−C(9)−O(3)	110.2(5)
		O(2)−C(9)−C(11)	117.1(5)
		O(3)−C(9)−C(11)	106.0(4)
		O(3)−C(9)−C(13)	97.7(4)
		C(11)−C(9)−C(13)	108.5(5)

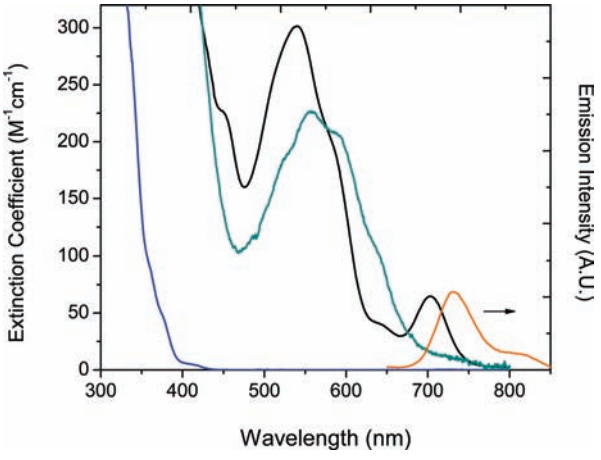

Figure 8. UV−vis absorption spectra of **A** (black), **B1** (green), and 10-hydroxyanthrone (blue) in CH_2Cl_2 at room temperature, and emission spectrum of a degassed CH_2Cl_2 solution of **A** (orange, excitation wavelength = 600 nm).

trans-influence of the carbanion is stronger than the alkoxide ion in the ketal group. The central ring of the anthrone shows a boat conformation whereby the O(3) is in the axial position. The anthrone ring in **B1** is severely bent, showing a dihedral angle of 43.6° between the two lateral aromatic rings. The C(9) and C(10) atoms of the central ring deviated from the other four C atoms in the

Scheme 2

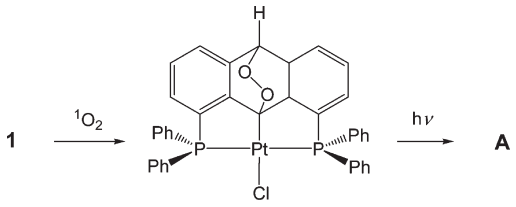

Pt-EP

central rings by 0.659 and 0.335 Å, respectively. The highly distorted coordination geometry of the Pt ion and anthrone ring suggests that **B1** is more strained than **A**.

Electronic Spectroscopy of A and B1. In contrast to the yellow color of **1**, **A** and **B1** are deep red in color. The absorption spectra of the complexes show a weak, low energy absorption band in ~450−700 nm (Figure 8). The energies and intensities of the absorption bands are similar: the absorption maxima ε_{max} (M^{-1} cm^{-1}) for **A** and **B1** are 540 nm (302) and 555 nm (226), respectively. The bands show weak vibronic features. In contrast, 10-hydroxyanthrone shows a weak shoulder at 402 nm and does not absorb at >430 nm.

It has been established that the lowest energy spin-allowed transition of anthrones is $^1n\rightarrow\pi^*$(C=O, phenyl rings).[21] The low intensities of the 540 and 555 nm absorption bands of the complexes are in accord with the orbital forbidden nature of $^1n\rightarrow\pi^*$ transition. Both complexes display very weak absorption in 670−750 nm. The absorption of **A** is most intense and distinct, showing a peak at 706 nm (ε_{max} = 64 M^{-1} cm^{-1}). It is tentatively assigned to the spin-forbidden $^3n\rightarrow\pi^*$ transition as the lowest energy excited states of aromatic ketones such as benzophenone and anthrone have been shown to be $^3n\pi^*$.[21a] Degassed solution of **A** exhibits a weak emission at 732 nm (Φ_{em} = 3 × 10^{-3}). The very small Stokes shift between the emission and the $^3n\rightarrow\pi^*$ absorption (~500 cm^{-1}) suggests the luminescence is derived from the $^3n\pi^*$ excited state.

Mechanistic Postulate. 10-Hydroxylanthrone (Scheme 1), one of the products of photooyxgenation of anthracene, arises from photoinduced homolytic cleavage of the peroxidic bond in the primary photoproduct 9,10-endoperoxide (**EP**) followed by rearrangement. That the hydroxyanthrone complex **A** is formed in the photooxygenation of **1** argues strongly that a Pt^{II}-endoperoxide complex (**Pt-EP**, Scheme 2) is formed in the reaction between oxygen and **1**.

It is possible that the **Pt-EP** is produced from reaction of **1** and $^1O_2$, as in the case for **EP**. The involvement of $^1O_2$ is evident from the fact that bleaching of the $\pi\rightarrow\pi^*$ band is faster in $CDCl_3$ than in $CHCl_3$ (Figure 9). The observation is in accord with the fact that the lifetime of $^1O_2$ in $CDCl_3$ (300 μs) is longer than in $CHCl_3$ (30 μs).[22] The $^1O_2$ could arise from photosensitization of the ground state O_2 by the excited state of **1**. The **Pt-EP** was not observed in the NMR spectrum of the photolyzed solution,

(21) (a) Lipson, M.; McGarry, P. F.; Koptyug, I. V.; Staab, H. A.; Turro, N. J.; Doetschman, D. C. *J. Phys. Chem.* **1994**, *98*, 7504. (b) Hoffmann, R.; Swenson, J. R. *J. Phys. Chem.* **1970**, *74*, 415.

(22) Kearns, D. R.; Merkel, P. B.; Nilsson, R. *J. Am. Chem. Soc.* **1972**, *94*, 7244.

Scheme 3

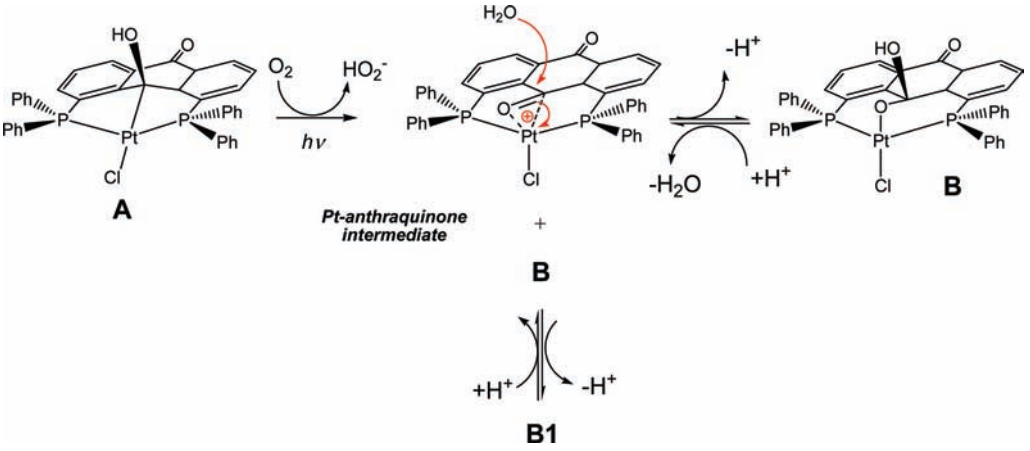

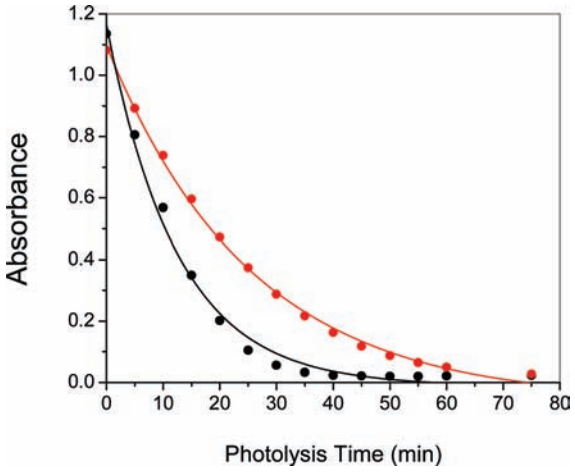

Figure 9. Absorbance of 452 nm band at different time of photolysis of **1** in aerated $CHCl_3$ (red) and $CDCl_3$ (black).

indicating that conversion from **A** to **Pt-EP** is fast and efficient.

In view of facile acid-catalyzed ketalization of hemiketal, we believe that the diketal **B1** originates from dimerization of a hemiketal **B**. On the basis of the well-established mechanism for ketalization,[23] a mechanism for the formation of **B** and **B1** is postulated (Scheme 3). First of all, in the presence of HCl, which is a common side product in photochemical reactions in chloroform,[24] a water molecule is eliminated from **B** to generate a Pt^{II}-anthraquinone intermediate which consists of a Pt^{II}-$(\eta^2$-O=C$)^+$ π-bonding.

It is noted that Milstein et al. reported an isoelectronic Ir^I pincer complex that exhibits Ir^I-$(\eta^2$-O=C) quinonoid coordination mode.[25] Nucleophilic attack of the hydroxyl group of another molecule of **B** at the electrophilic Pt^{II}-$(\eta^2$-O=C$)^+$ unit of the intermediate would lead to **B1**.

Light can accelerate the oxidation of **A** to **B** conversion. In one experiment, an aerated solution of **A** was divided into two parts, one was exposed to visible light while the other was kept in darkness. The $^{31}P\{^1H\}$ NMR spectrum of the solution irradiated for 2 days indicated 85% conversion whereas only 6% conversion was observed for the solution kept in darkness for *2 weeks*. The result demonstrates clearly that the oxidation of **A** to **B** is very slow but can be accelerated by photoexcitation. Examples of direct O atom insertion into transition-metal−carbon bond have been reported for some cyclometalated palladium complexes[26] but strong oxidant such as metal-peroxide or *t*-butyl hydroperoxide is needed to insert O atom into the Pd−C(sp^2) bond. Oxygenation of the metal-C(sp^3) in $(t\text{-}Bu_3CO)_2M(Me)_2$ (M = Ti, Zr, Hf)[27] involves direct insertion of O_2 to generate metal peroxides or alkoxides. However, for late transition metals, the reactions are limited to the first row and there is no example of direct insertion of O_2 into Pt−C bond to form Pt-alkoxide. Recently, Goldberg et al. showed direct insert of O_2 into Pt−C bond to form a Pt-alkylperoxide[28] but not a Pt-alkoxide as in the present case.

We proposed that the oxidation of **A** to **B** involves oxidation of the anthrone by oxygen to the Pt^{II}-anthraquinone intermediate which is the same as the one proposed for the ketalization of **B** (Scheme 3). Nucleophilic attack of H_2O at the intermediate gives rise to the hemiketal **B** (Scheme 3). The proposed mechanism can explain the fact that the oxidation can be accelerated by irradiation as the emissive excited state of **A** can sensitize conversion of ground state O_2 to $^1O_2$ which is more oxidizing than the former.

Conclusion

Photooxidation of the cyclometalated Pt^{II}-anthracene pincer complex leads to a Pt^{II}-9-hydroxyanthrone complex that can be further oxidized to a Pt^{II}-hemiketal complex. It is believed a Pt^{II}-9,10-endoperoxide complex is formed from the reaction between **1** and singlet oxygen. The Pt^{II}-hemiketal complex undergoes ketalization to form a Pt^{II}_2-diketal via a

(23) (a) Fife, T. H. *Acc. Chem. Res.* **1972**, *5*, 264. (b) Anslyn, E. V.; Dougherty, D. A. *Modern Physical Organic Chemistry*; University Science Books: Sausalito, CA, 2004, p 578.

(24) (a) Hoggard, P. E.; Bridgman, A. J.; Kunkely, H.; Vogler, A. *Inorg. Chim. Acta* **2004**, *357*, 639. (b) Hautecloque, S. *J. Photochem.* **1980**, *14*, 157.

(25) Vigalok, A.; Rybtchinski, B.; Gozin, Y.; Koblenz, T. S.; Ben-David, Y.; Rozenberg, H.; Milstein, D. *J. Am. Chem. Soc.* **2003**, *125*, 15692.

(26) (a) Alsters, P. L.; Boersma, J.; van Koten, G. *Organometallics* **1993**, *12*, 629. (b) Alsters, P. L.; Teunissen, H. T.; Boersma, J.; Spek, A. L.; van Koten, G. *Organometallics* **1993**, *12*, 4691.

(27) (a) Lubben, T. V.; Wolczanski, R. T. *J. Am. Chem. Soc.* **1987**, *109*, 424. (b) Brindley, P. B.; Hodgson, J. C. *J. Organomet. Chem.* **1974**, *65*, 57.

(28) Grice, K. A.; Goldberg, K. I. *Organometallics* **2009**, *28*, 953.

Pt^{II}-anthraquinone intermediate which is proposed as the intermediate in the oxidation of the Pt^{II}-9-anthrone to the Pt^{II}-hemiketal.

Acknowledgment. We thank Ms Tan Geok Kheng and Prof Koh Lip Lin for determining the X-ray crystal structures. Ministry of Education, Singapore (R-143-000-331-112) and National University of Singapore are thanked for providing financial support.

Supporting Information Available: CIF of **1**, **A**, and **B1**, X-ray crystal structures of **2** and **3**, and ^{1}H NMR spectra of photolysis of **1**. This material is available free of charge via the Internet at http://pubs.acs.org.